CHAPTER 4: ESTIMATING BIOPHYSICAL AND BIOCHEMICAL PARAMETERS FROM A HALF RANGE PSUEDO HYPERSPECTRAL IMAGE GENERATED FROM UAV IMAGERY

4.1 INTRODUCTION

LCC is a biochemical property of a vegetation that determines health of any vegetation, it changes at different phenological stages and it is affected when exposed to certain types of stresses by determining any change in vegetation's pigment level. Thus, its study would help agronomists to take precautionary measures to improve the yield of crop at critical stages [59]. The visible part of vegetation's EM spectrum is dominated by chlorophyll content. Chlorophyll pigments have a low reflectance in the visible spectrum's red and blue bands [60]

LAI is a biophysical parameter of any vegetation that explains the interaction of radiation with the vegetation. Mathematically, it is explained as leaf area (m^2) per unit ground area (m^2), making it a dimensionless quantity [26]. LAI is a useful property to asses local and global ecosystems, and in calculating the photosynthetic capacity of vegetation [61]. It is also critical parameter to estimate foliage cover, monitor, and forecasting growth and yield of the crop. Thus, extensive inspection of LAI is an important aspect in agroecological and climatic study [62, 63]. Measuring crop biophysical and biochemical parameters is critical for detecting seasonal changes. Furthermore, to determine whether or not yield quality has improved and what more could be done to better its quality [27, 64]

Different sensors mounted on satellites and UAV are now available to acquire spectra of vegetation to help with such goals. Satellite's sensors retrieve data in the electromagnetic spectrum ranging from visible to microwave region in the form of multispectral and hyperspectral sensors with different spectral resolutions. In order to retrieve information that requires fine spectral information, multispectral images fail to provide that, but they provide global information with easy availability. Whereas, hyperspectral images with rich spectral resolution are not freely available. So, many researchers worked on the idea to use the availability of multispectral image information to generate pseudo hyperspectral images which are free of cost, and fulfils the purpose of an original hyperspectral image [38].

One such spectral reconstruction method that is sensor independent is UPDM [52] which is a modified form of Pattern Decomposition Method. In this technique, reflectance of pixel can be decomposed as the linear combination of classes present in it. There are studies that uses UPDM to generate hyperspectral images using multispectral images in different domains [65].

Although, the spatial resolution of image generated using such method is limited to the spatial resolution of multispectral image which is not necessarily better than the hyperspectral image [53]. So, to simulate such image with very good spatial and spectral resolution, we need a multispectral image of very fine spatial resolution which is only possible if we have an image acquired from a relatively lower altitude which is possible by UAV.

In the presented work, using SRF of RedEdge MX and AVIRIS-NG, a half range hyperspectral imagery was simulated with 105 bands. To validate the authenticity of the simulated image, LCC and LAI of few vegetation were retrieved and compared using ground truth data.

4.2 METHODOLOGY

4.2.1 Study area and data acquisition

A rigorous field sampling was done over a part of agricultural farm present in BHU, Varanasi on March 14, 2022, around 12:00 pm (Figure 2.9 a), the reason for choosing the time is mentioned in Section 1.9. Figure 4.1 is an RGB image acquired from the UAV, during this sampling, LCC and LAI of different types of vegetation were recorded. LAI and LCC observations were done with the help of LAI-2200C plant canopy analyser and SPAD respectively. In order to generate spectral library for the vegetation types, FieldSpec 4 a spectroradiometer was used to take the leaf level spectral radiance. The workflow of the current study is similar to Figure 3.1, Section 3.2.1.

Figure 4.1. RGB image of study site taken from RedEdge MX

4.2.2 Aerial image acquisition

Aerial imageries were acquired using Micasense RedEdge MX multispectral sensor (Figure 2.4 a) onboard a Lookout VTOL – Lite (Throttle Aerospace Systems, Bangalore, India) RPAS with a real-time kinematic (RTK) receiver (Figure 2.4 b). The detailed specifications of the UAV and sensor are provided in Table 4.1. The image acquisition was done on March 14, 2022 in calm wind and clear weather conditions, keeping the front and side overlap at 70%, above-ground flight height at 60m, and cruise speed at 6m/s, resulting in a GSD of ~4.2 c. The planning of mission was done manually using the TAS mission planner.

The AVIRIS-NG SRF data was used (Chapter 3, Section 3.2) in the current investigation to generate half range AVIRIS-NG equivalent image using drone data.

Table 4.1 Specifications of UAV and RedEdge MX

<table>
<tr><th>S. No.</th><th colspan="2">Lookout VTOL – Lite</th><th colspan="2">Micasense RedEdge MX</th></tr>
<tr><td>1</td><td>Category and weight</td><td>MICRO, 1.995 Kg</td><td>Weight</td><td>150 g
(231.9 g with
DLS and cables</td></tr>
<tr><td>2</td><td>Type</td><td>Quadcopter</td><td>Dimensions</td><td>12.1 cm x 6.6 cm x 4.6 cm (4.8” x 2.6” x 1.8”)</td></tr>
<tr><td>3</td><td>Dimensions</td><td>900 x 900 x 300mm</td><td>Spectral Bands</td><td>Blue, Green, Red, Red Edge, Near IR (global shutter, narrowband)</td></tr>
<tr><td>4</td><td>Operating altitude</td><td>Altitude 120m, VLOS</td><td>GSD</td><td>8.2 cm/pixel (per band) at 120 m (400 ft.) AGL</td></tr>
<tr><td>5</td><td>Cruise Speed</td><td>6 m/s, Max: 10 m/s</td><td>Capture Speed</td><td>1 capture per second (all bands), 12-bit RAW</td></tr>
<tr><td>6</td><td>Wind tolerance</td><td>up to 12 m/s</td><td>Field of View</td><td>47.2° FOV</td></tr>
<tr><td>7</td><td>Payload</td><td>Multiple (RGB, EOIR, MS, Radiometric)</td><td>Wavelength (nm)</td><td><table>
<tr><th></th><th>Band Name</th><th>Wavelength (nm)</th><th>Bandwidth (nm)</th></tr>
<tr><td>1</td><td>Blue</td><td>475</td><td>20</td></tr>
<tr><td>2</td><td>Green</td><td>560</td><td>20</td></tr>
<tr><td>3</td><td>Red</td><td>668</td><td>10</td></tr>
<tr><td>4</td><td>NIR</td><td>840</td><td>40</td></tr>
</table></td></tr>
</table>

5	Red Edge	717	10

4.2.3 Simulating a pseudo hyperspectral imagery using SRF of AVIRIS-NG and RedEdge MX:

4.2.3.1 Computing standard spectra

The major portion in experimental site contains agricultural fields, bare soil, and harvested land, as shown in Figure 4.2, since in UPDM, we have to give three endmember classes with different spectra, so bare soil and harvested land were considered under one spectra of soil class. Therefore, three primary endmembers, matured crop, vegetation, and soil was chosen to be given to the algorithm. The spectra of the classes were taken during the data sampling.

The standard spectra of each class, i.e., matured crop, vegetation, and, soil, were calculated as mentioned by the method described in Chapter 3, Section 3.2.3.1 [65, 66].

4.2.3.2 Spectral unmixing

As explained in the Chapter 3, UPDM is a sensor independent spectral reconstruction method used for the image simulation. The three major classes given to UPDM to generate the half range AVIRIS-NG image, for the current study, are green vegetation, matured crops, and soil. The green vegetation class, covers agricultural crops, identified during field sampling. Soil covers bare and harvested land cover. Whereas matured crops were taken as the third class. Thus, equation 3.3 becomes

$$R_i = P_{iv}C_v + P_{is}C_s + P_{imc}C_{mc} \qquad (4.1)$$

Here, C_v, C_s, and C_{MC} are the decomposition coefficients, and P_{iv}, P_{is}, and P_{imc} are normalized standard spectra for green vegetation (v), soil (s), and matured crop (MC), respectively.

For n number of bands equation 4.1 takes a matrix form, shown as

$$\begin{pmatrix} R_1 \\ R_2 \\ \vdots \\ R_n \end{pmatrix} = \begin{pmatrix} P_{1v} & P_{1s} & P_{1mc} \\ P_{2v} & P_{2s} & P_{2mc} \\ \vdots & \vdots & \vdots \\ P_{nv} & P_{ns} & P_{nmc} \end{pmatrix} \begin{pmatrix} C_V \\ C_S \\ C_{MC} \end{pmatrix} \tag{4.2}$$

For RedEdge MX, right hand side of Equation 4.2 would be of dimension 5×1, whereas for the half range simulated AVIRIS-NG it should be 105×1.

Further, resultant HIS equivalent to AVIRIS-NG was generated using calculations from using calculations from equation numbers 3.6, 3.7, 3.8, and 3.9.

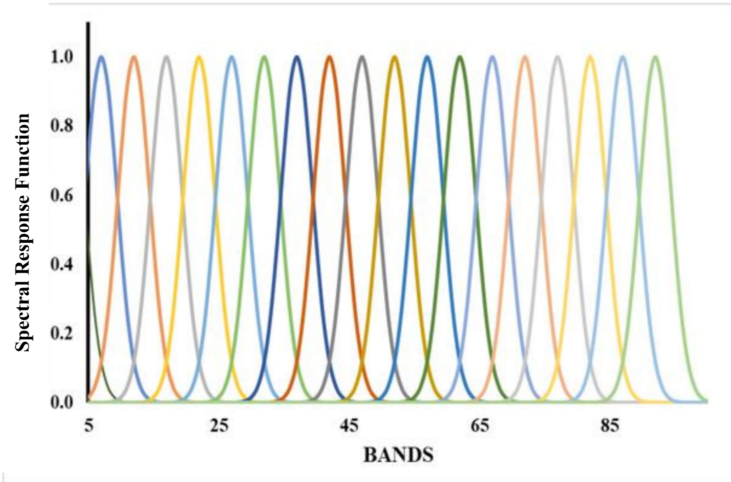

(a)

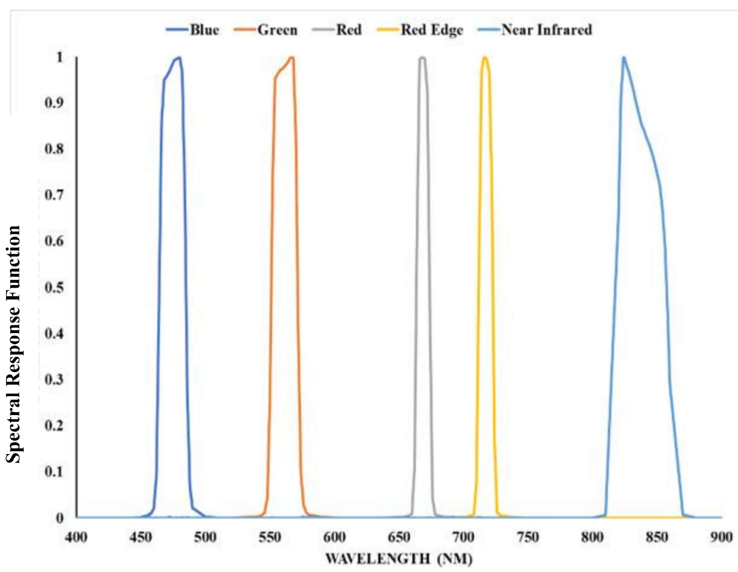

(b)

Figure 4.2 (a & b). SRF of AVIRIS NG sensors and RedEdge MX

4.3. RESULTS AND DISCUSSION:

4.3.1 Simulation of half range AVIRIS-NG:

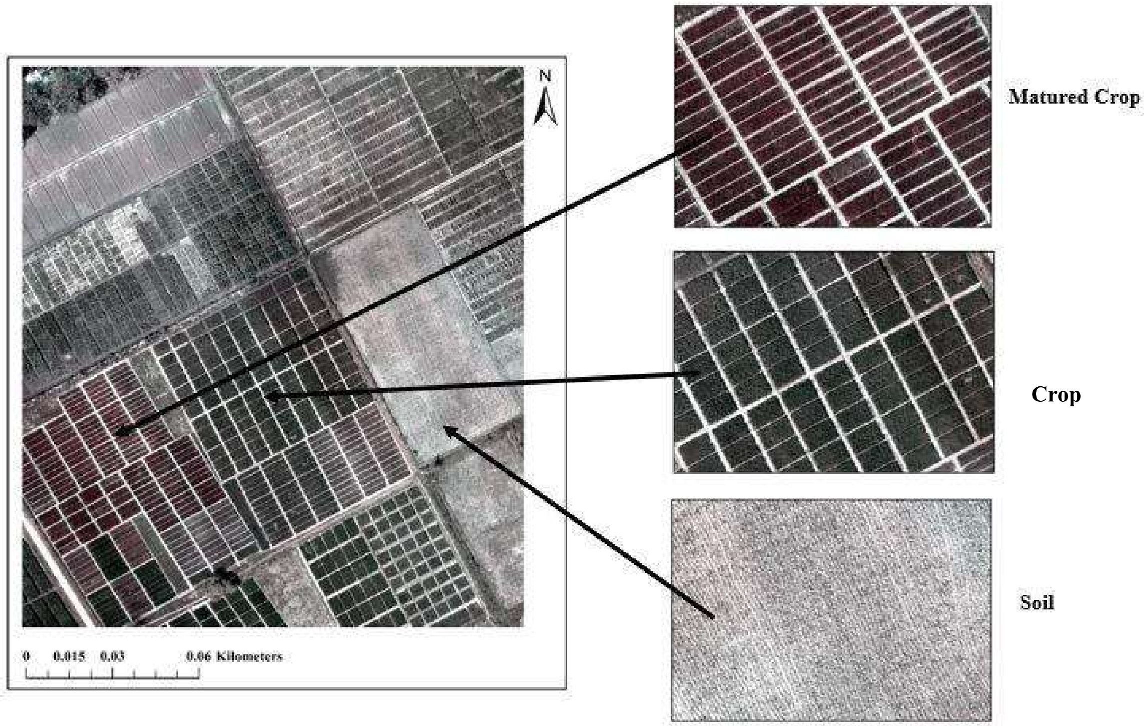

Figure 4.3. Simulated half range hyperspectral image (380-1000 nm)

In the present work a half range AVIRIS-NG image was simulated using a UAV image and a linear spectral unmixing technique. Figure 4.1 is the UAV image acquired for the study area, it is observed that the cropbed contains mainly various crops at different growth stages along with bare and harvested lands, Figure 4.3 is the simulated image for the same. Since UPDM, is a sensor independent technique, spatial resolution of simulated image would remain as that of multispectral image used for the simulation. Therefore, the image generated has the spatial resolution of 4.2cm, which is ten times better than the original AVIRIS-NG image. However, there are 425 bands in AVIRIS-NG image, but since we are working with five bands of RedEdge MX i.e. blue, green, red, red edge and NIR, we are bound to expand it to only till NIR region. The image simulated has 105 bands starting from visible to NIR bands with spectral resolution of

5nm and a spatial resolution of 4.2cm. From Figure 4.3, it is found that the image can visually distinguish between different stages of crops, matured crop is reddish in colour whereas vegetative are in green colour, dry and wet soil are also easily distinguishable. The resultant image was further scrutinized for the estimation of vegetation parameters.

4.3.2 LAI\LCC retrieval and mapping:

In order to check the usability of image simulated, LAI and LCC for few vegetation species were retrieved from the simulated image which was compared with the in-situ values. Vegetation indices based linear models [55, 67] were calculated for the retrieval of LAI and LCC are, shown by Equations 4.3 and 4.4;

$$NDVI = \frac{R_{800}-R_{680}}{R_{800}+R_{680}} \tag{4.3}$$

$$CCI14 = \frac{R_{686}-R_{556}}{R_{686}+R_{556}} \tag{4.4}$$

where, R_i is the reflectance value in i^{th} band, here i^{th} bands are band number 800, 680, 686, and 556 bands.

4.3.3 Performance indices:

The performance of the estimation of vegetation parameters from the simulated image have been eavaluated using R and RMSE given by Equations (4.5) and (4.6);

$$R = \left[\frac{\frac{1}{n}\sum_{i=1}^{n}(f_{obs} \cdot f_{pred})}{\sigma_{obs} \cdot \sigma_{pred}}\right] \tag{4.5}$$

$$RMSE = \sqrt{\frac{\sum_{i=1}^{n}(f_{obs}-f_{pred})^2}{n}} \tag{4.6}$$

where, f_{obs} and f_{pred} are ground truth data and predicted value, where as σ_{obs} and σ_{pred} are standar deviation of ground truth and predicted data.

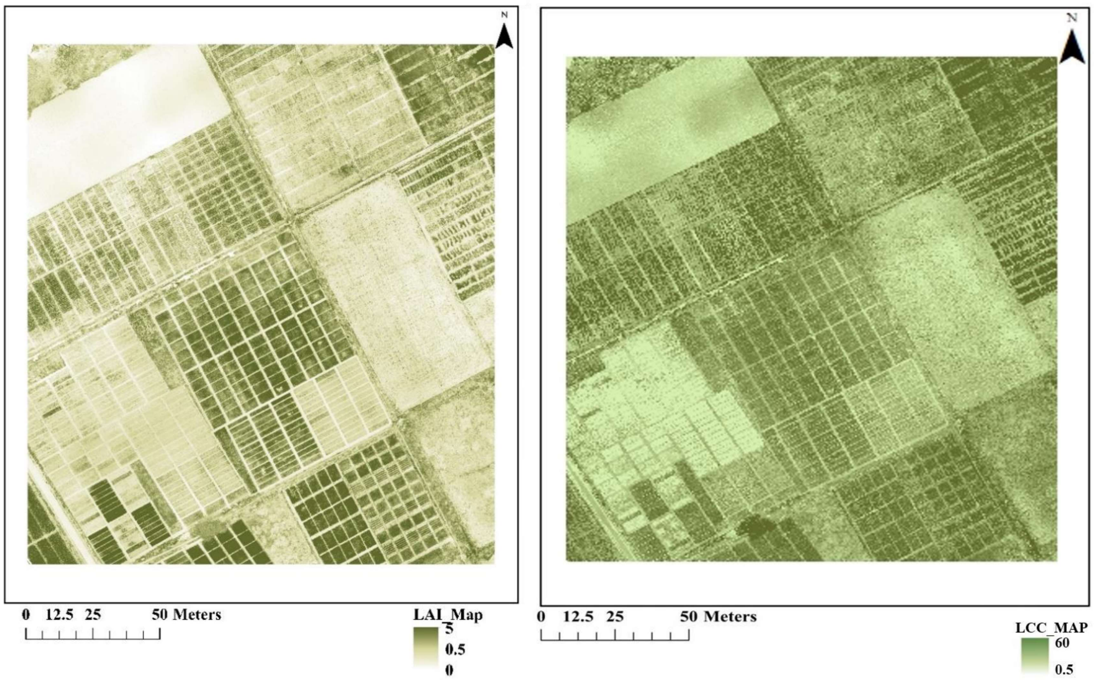

(a) (b)

Figure 4.4 (a & b). LAI and LCC maps for the study site (left and right, respectively)

LAI Estimation

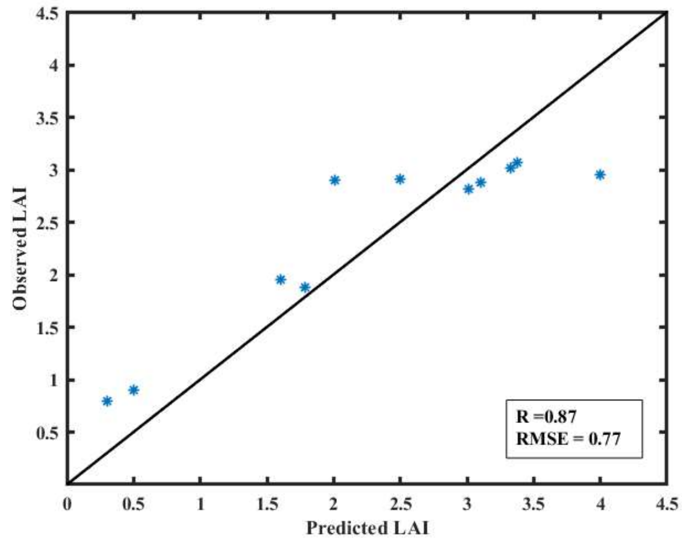

LCC Estimation

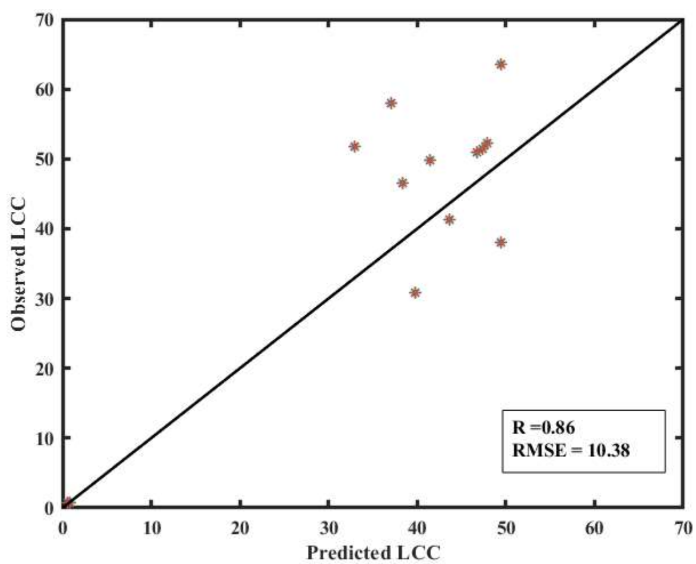

Figure 4.5. Comparison of estimated LAI and LCC w.r.t. observed values

After generation of half range pseudo hyperspectral image (HRPHSI) for the study area using drone data, its usability was checked for the estimation of LAI and LCC, and then maps were generated further (Figures 4.4 a and b, respectively). LAI value range was retrieved between 0 to 5 and LCC values range were retrieved between 0 to 60. Few in-situ LCC and LAI were recorded during data sampling which was compared with the estimated parameters calculated from VI based linear models derived from the map. This comparison is illustrated in Figure 4.5. It is observed from the figure that the R value and RMSE value for LAI and LCC estimation was found out to be (0.87; 0.77) and (0.86; 10.38), respectively. According to results it is observed that simulated image was performing well during the comparison between simulated and measured values of LAI and LCC.

4.4. CONCLUSIONS

In the present work, a HRPHSI was generated for a UAV based multispectral camera image (RedEdge MX) image using SRF of the camera image and AVIRIS-NG. The RedEdge MX contains only five bands, that is why the hyperspectral image simulation was restricted to 1000 nm. By observing the HRPHSI, it was found that by increasing the spatial resolution the LCC & LAI estimation accuracy was increased despite of restrictions in the number of bands compared to earlier parameters estimation studies (mentioned in Chapter 3).

Although, from this method we simulated a half range AVIRIS-NG image, but for vegetation purpose we would also require SWIR bands, as it gives information of water absorption bands and hence the amount of water present in it. To correct this situation, we may add few more sensors of SWIR bands to the UAV, however this is instrumentation issue but if accomplished we will have a full range hyperspectral image with rich spectral as well as spatial resolution. Although increasing three or four sensors might increase the cost of the system but it would still be very much low compared to the cost of mounting hundreds of sensors of a hyperspectral camera.

If mount more sensors suitable to payload, can be mounted on the UAV, then the generated image would be so fine that it will be equivalent to a ground-based data but with spectral richness of a hyperspectral image. Compared to ground data measuring this image would have large coverage, thus the image generated would have best of both airborne coverage and ground based spatial precision with high spectral resolution.